

Protection of Computer Enclosure against Coupled Electromagnetic Interference

Run Xiong¹, Wen Yang², Hai-Lin Chen³, and Yan-Tao Duan³

¹ PLA Army Engineering University, Xuzhou, Jiangsu, China
xiongrun1983@sina.com

² Army Research Institute of PLA, Kunming, Yunnan, China
76077381@qq.com

³ PLA Army Engineering University, Nanjing, Jiangsu, China
hylinchen@126.com, yantaoduan@sina.com

Abstract — In this paper some suggested protection methods is proposed to improve the shielding effectiveness of computer enclosures. Slots and holes on the computer enclosure are divided into five types, and the coupled electromagnetic interference (EMI) into the enclosure is computed using the finite-difference time-domain (FDTD) method when each type slot exists. From comparison of both time domain electric field waveform and field distribution in the enclosure, vent array, joint laps, CD-ROM and display are found to be the main ways that the EMI penetrated into the enclosure. To improve the protection of the enclosure, waveguide window is used to replace vent array. Additionally, rivet number is increased, depth of the joint laps is increased and conductive gaskets are filled into the joint laps. From numerical analyses, it can be demonstrated that the suggested methods are efficient to improve shielding effectiveness of the computer enclosure. Some suggested methods are also proposed for the CD-ROM and display protection.

Index Terms — Electromagnetic interference (EMI), finite-difference time-domain (FDTD), shielding effectiveness (SE).

I. INTRODUCTION

With the development of the electronic technology, electronic equipment requires to work in a quiet electromagnetic environment. Electromagnetic shielding is frequently used to reduce electro-magnetic interference (EMI) of electronic equipment [1-2]. Shielding computer enclosure is an effective way to diminish the EMI [3-4]. However, in most applications, slots, holes, and even a window aperture have to be created on the walls of the computer enclosure for signal wiring, power supply, display, etc. These slots, unfortunately, provide electromagnetic energy coupling paths that allow outside

electromagnetic waves to propagate into the enclosure; they thus degrade the shielding effectiveness (SE). Therefore, it is necessary to analyze SE of the shielding enclosures. EMI introduced into the enclosure by lines are as serious as that by coupling, however, only the EMI introduced by coupling are considered here.

The finite-difference time-domain (FDTD) method [5-11], which provides a simple and efficient way of solving Maxwell equations for a variety of problems, has been widely applied in solving many types of electromagnetic coupling problems. It is good at predicting the SE of a particular enclosure for it has numerous time-domain and frequency-domain information.

To simulate the EMI coupled into the computer enclosure, high power microwave (HPM) is used as the source. Total-field/scattered-field (TF/SF) boundary [5] is used to introduce the HPM. Convolution Perfectly Matched Layer (CPML) [12-13] absorbing boundary, which is good at solving late-time reflects, is used to truncate the computational domain. Considering that the EMI mainly penetrates into the enclosure through apertures rather than that through the walls, the perfect electric conducting plane is used to model the shield enclosure.

To find the main ways that EMI coupled into computer enclosure, the slots on computer enclosure are divided into five types and the coupled EMI into the enclosure is studied when each type slot exists. From comparison of both the electric field waveform and the field distribution in the enclosure, vent array, joint laps, CD-ROM and display are found to be the main ways that the EMI coupled into the computer enclosure.

To diminish coupled EMI into the enclosure, light transmitting and electromagnetic wave shielding composite materials can be used to produce the CD-ROM shell and display screen [10-11]. Waveguide

window is used to take place of vent array. Additionally, rivet number is increased, the depth of the joint lap is increased and conductive gaskets are filled into the joint laps. From numerical analyses, it can be seen that the suggested programs are efficient to improve SE of the computer enclosure. Only methods to reduce the coupled EMI through vent array and joint laps are studied here.

II. THE COMPUTATIONAL MODEL

To be simply, an industrial control computer enclosure is involved here, as shown in Fig. 1, where the slots on both front and back faces are also graphed. The enclosure is made up of bonding the metal sticks together, thus there are joint laps at the top of the four side surfaces.

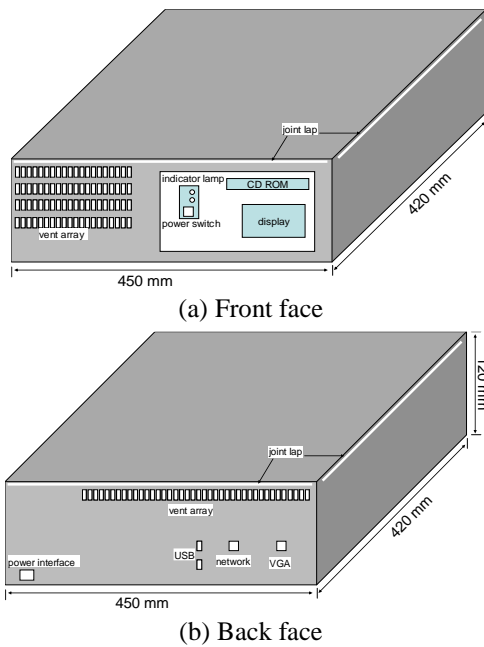


Fig. 1. Various slots on computer enclosure.

HPM is used as the source here, whose waveform is graphed in Fig. 2. Here it is set,

$$E_0 = \begin{cases} 2.5 \times 10^5 \text{ V/m} & f \leq 10\text{GHz} \\ 2.5 \times 10^6 / f(\text{GHz}) \text{ V/m} & f > 10\text{GHz} \end{cases} \quad (1)$$

It is set $50 \text{ ns} < \tau < 10 \text{ } \mu\text{s}$, $t_1 = 10 \text{ ns}$, and the repeat frequency is 1 kHz. The peak power of the HPM is:

$$P_{pk} = \begin{cases} 100 \text{ GW} & f \leq 10\text{GHz} \\ 10^4 / f^2 \text{ GW} & f > 10\text{GHz} \end{cases} \quad (2)$$

The slots on the computer enclosure can be divided into five types, that is CD-ROM and display, vent array on the two faces, joint laps at the top of four enclosure side surfaces, power line and signal interfaces (containing slots for power line interface, USB, network, and VGA), the power switch and indicator light.

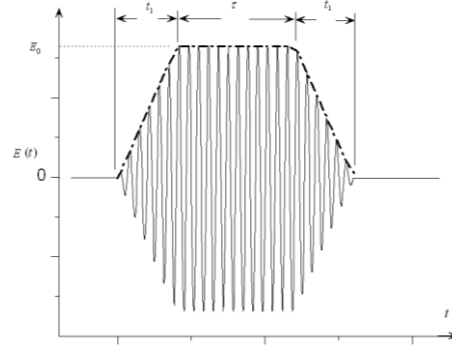


Fig. 2. Waveform of the HPM.

The SE used throughout the paper is given by:

$$SE = -20 \log \left(\frac{|\bar{E}^{shield}|}{|\bar{E}^{inc}|} \right), \quad (3)$$

where, \bar{E}^{shield} refers to the electric-field value when computer enclosure is placed, whereas \bar{E}^{inc} refers to the electric-field value at the same location in the absence of the enclosure.

To evaluate the SE of the enclosure, all the three directional electromagnetic fields at the center of the enclosure is monitored first, and the waveform of the largest field direction is graphed. Additionally, the peak field value of the waveform is recorded and used to derive the total electric field component:

$$E_p(t) = 20 \log \left[\sqrt{E_x(t)^2 + E_y(t)^2 + E_z(t)^2} \right] \text{ dBV/m} \quad (4)$$

To improve the protection of the enclosure, the coupled EMI into the enclosure is simulated when only one type of slot exists to find the main ways that the interface coupled into the computer enclosure. Then some suggested methods are proposed to limit the coupled EMI, and numerical simulation is occupied to verify the efficiency of these methods.

Cubic FDTD cells are used in this paper, and the cell size is $\Delta = 0.5 \text{ mm}$ in three directions. To satisfy the stability condition of the FDTD algorithm, the maximum time step is chose to be $\Delta t = \Delta / 2c$, where c is the speed of light in the free space. The computational domain is truncated by 10-layers CPML absorbing boundary.

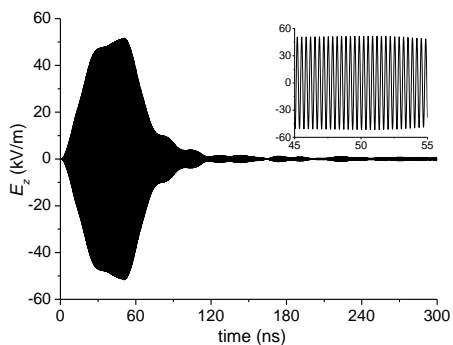
III. ANALYSES OF THE COUPLING WAYS

To find the main ways that EMI coupled in, the computational enclosure is illuminated by HPM when only one type of slot exists. The coupled electric field component into the enclosure in the three directions is monitored respectively, and time-domain waveform of the largest one is drew. Additionally, distribution of the largest total electric field component is also graphed. From analysis of the electric field component coupled into the enclosure when the five types of slots exist

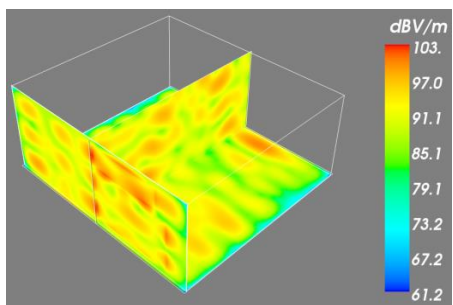
lonely, and the main way that EMI coupled into the enclosure is identified.

A. Slots for CD-ROM and display

In this part the coupled EMI is studied when only the CD-ROM and display slots exist. The CD-ROM slot is 15 cm in length and 4 cm in width, and the slot dimension of the display is 17 cm×10 cm. The slot dimension of the CD-ROM and display is larger than the EMI wavelength, and these slots are modeled by standard FDTD grids. Both the CD-ROM and display slots are located on the front face of the enclosure. After FDTD simulation, both the electromagnetic field and the field distribution are monitored.



(a) Time-domain waveform



(b) Field distribution

Fig. 3. EMI coupled through CD-ROM and display.

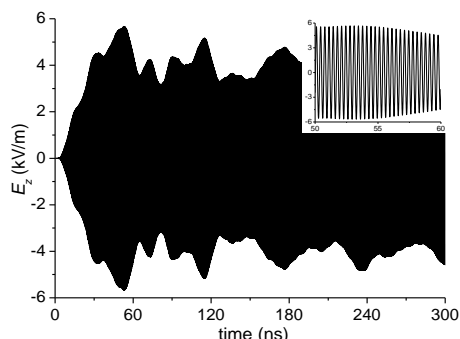
The amplitude of the electric field component field E_x is 25.5 kV/m, and field component amplitude is 13.2 kV/m for E_y and 51.4 kV/m for E_z respectively. In Fig. 3 (a) is graphed the waveform of the electric field component E_z , and the waveform at the right up corner is the 10 ns waveform near the maximum amplitude. It can be seen that the electric field coupled into the enclosure is very large and decreased rapidly.

In Fig. 3 (b) is graphed the total electric field distribution in the enclosure. It can be seen that the electric field is larger than 61.2 dBV/m throughout the enclosure, and even reaches 103 dBV/m at some places, and the electric field is larger than 85 dBV/m at most places in the enclosure. Thus, it can be concluded that the enclosure can rarely shield HPM when CD-ROM and

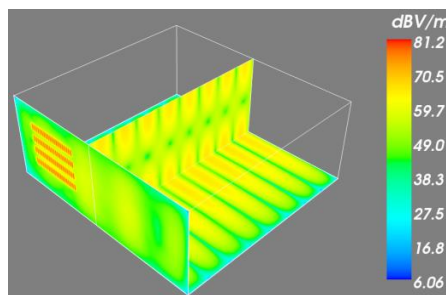
display exist on the enclosure.

B. Slots of vent array on the two faces

In this part the coupled EMI is studied when only the slots for vent array on the two faces exist. The vent array is composed of 4 lines of slots, and each line is composed of 20 thin-slots. The size of each slot is the same, with the dimension of 1.5 cm in height and 0.3 cm in width. The distance between left thin-slot and the right one is 0.3 cm, and the distance is 1.0 cm from the up thin-slot line to the down one. The dimension of the vent array is 12 cm×10 cm.



(a) Time-domain waveform



(b) Field distribution

Fig. 4. EMI coupled through vent array.

The dimension of the thin-slots of the vent array on the back face is the same as those on the front face. The vent array on the back face is in one line and consists of 40 thin-slots. The distance between the two thin-slots is 0.3 cm, and the dimension of the vent array is 24 cm×1 cm. From FDTD simulation, both the time-domain electric field component and the field distribution are monitored, as graphed in Fig. 4.

The amplitude of the electric field component E_x is 1.3 kV/m, and field component amplitude is 2.2 kV/m for E_y and 5.7 kV/m for E_z respectively. In Fig. 4 (a) is graphed the waveform of E_z , and the waveform at the right up corner is the 10 ns waveform near the maximum amplitude. It can be seen that the electric field coupled into the enclosure is also large. It can also be seen that resonance occurs in the enclosure and the amplitude decreases very slowly.

In Fig. 4 (b) is graphed the total electric field distribution in the enclosure, and it is clear that the four lines of slots are conspicuous on the enclosure. It can also be seen that a resonance occurs in the enclosure and the coupled electric field is much lower compared with that when the CD-ROM and display exist. The amplitude of the electric field varies from 6.06 dBV/m to 81.2 dBV/m in the enclosure, and the amplitude is larger than 50 dBV/m at most areas. Thus, it can be concluded that the SE of the enclosure is limited when vent arrays exist on the two faces of the enclosure.

C. Slots of joint laps

In this part the coupled EMI is studied when only the slots for joint laps exist. The joint lap is located on the top of the enclosure, as shown in Fig. 5. The width of the joint laps is 0.5 mm, and the depth is 1.0 cm. The length of the joint laps is the same as the side perimeter of the enclosure. The joint lap on each side is divided into 3 parts by 2 rivets. After FDTD simulation, both the electromagnetic field and the field distribution are monitored, as graphed in Fig. 6.

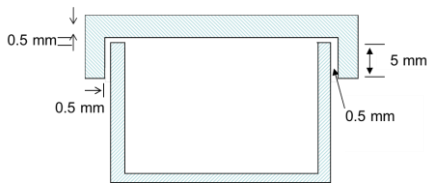
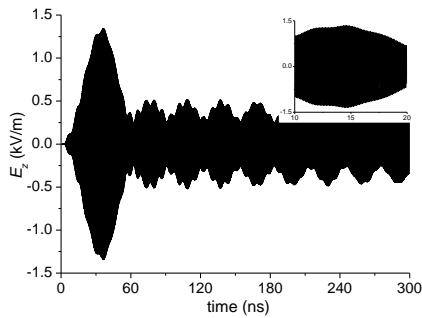
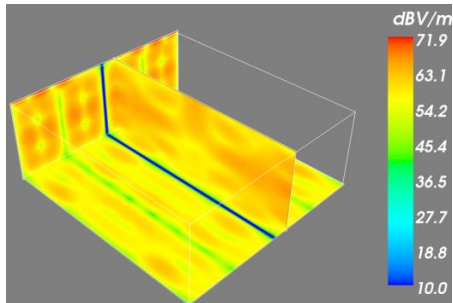


Fig. 5. The joint lap on the enclosure



(a) Time-domain waveform



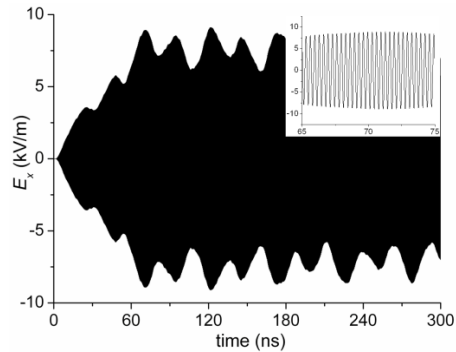
(b) Field distribution

Fig. 6. EMI coupled through joint laps.

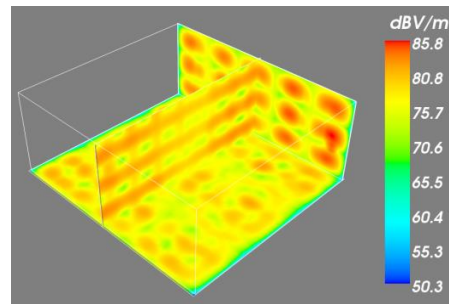
The electric field component E_x is very low and even can be neglected, and the field component amplitude is 0.56 kV/m for E_y and 1.3 kV/m for E_x respectively. In Fig. 6 (a) is graphed the time-domain waveform of the electric field component E_z , and the waveform at the right up corner is the 10 ns waveform near the maximum amplitude. In Fig. 6 (b) is graphed the total electric field distribution in the enclosure. It can be seen that the amplitude of the electric field varies from 10.0 dBV/m to 71.9 dBV/m in the enclosure, and the amplitude is about 50 dBV/m at most areas.

D. Slots of power line and signal interfaces

In this part the coupled EMI is studied when only the slots for power Line and signal interfaces exist. The signal interfaces is composed of universal serial bus (USB), network and video graphics array (VGA). There are two slots of USB, one slot of network and VGA, and these slots are all located on the back face of the enclosure. The width of the USB slot is 1.5 cm, and the height is 0.6 cm. The network slot is 1.5 cm in width and 1.0 cm in height. The dimension of the VGA slot is 2.5 cm×2.0 cm.



(a) Time-domain waveform



(b) Field distribution

Fig. 7. EMI coupled through slots of power line and signal interfaces.

The amplitude of the electric field component E_x is 9.0 kV/m, and field component amplitude is 1.3 kV/m for E_y and 5.5 kV/m for E_z respectively. In Fig. 7 (a) is graphed the time-domain waveform of the electric field component E_x . It can be seen that the coupled electric

field component E_x is much larger than other slots; resonance occurs in the enclosure and the amplitude decreases very slowly.

In Fig. 7 (b) is graphed the total electric field distribution in the enclosure. It can be seen that the coupled electric field in the enclosure is more uniformly distributed in the enclosure than other types of slots. The amplitude of the electric field varies from 50.3 dBV/m to 85.8 dBV/m in the enclosure, and the amplitude is larger than 80 dBV/m at most areas.

E. Slots for power switch and indicator lamp

In this part the coupled EMI is studied when only the slots for power switch and indicator lamp exist. The slot of the power switch is a square one with the width of 1 cm in each side. There are two indicators, one for power and another for hard disk. The slots of the two indicator lamp are all round holes, whose radius is 2 mm. Both the power switch and the two indicator lamp are located on the front face of the enclosure.

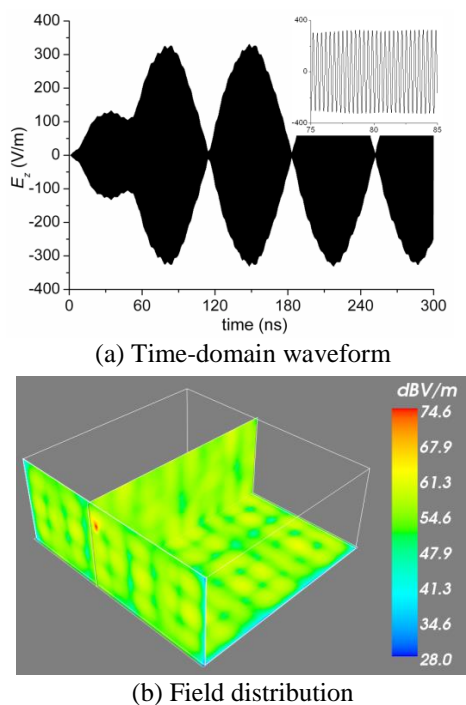


Fig. 8. EMI coupled through slots of power switch and indicator lamp.

The coupled EMI is much lower than that when the other types of slots exist. The amplitude of the electric field component field E_x is 0.36 kV/m, and field component amplitude is 0.13 kV/m for E_y and 0.33 kV/m for E_z respectively. In Fig. 8 (a) is graphed the waveform of the electric field component E_x , and it is clear that resonance occurs. The total electric field distribution in the enclosure is graphed in Fig. 8 (b), and the location of the power switch is obvious. It can be seen from Fig. 8

(b) that the amplitude of the electric field varies from 28.0 dBV/m to 74.6 dBV/m in the enclosure, and the amplitude is larger than 60 dBV/m at most areas. It is worthy of noting that the electric field near the slots is much larger than the other areas, and the effect of this type slots on the SE is limited.

From the coupled EMI analyses when only one type slots exist above, some conclusions can be drawn:

- (1) Joint laps, vent array, CD-ROM and the display are the main way that the EMI coupled into the enclosure.
- (2) Resonance occurs when the EMI coupled into the enclosure, and the resonant frequency is not only depending on the enclosure size but also the size of the slots.
- (3) The SE of the enclosure is limited when these types of slots exist, and the coupled electric field can even reach 103 dBV/m in the enclosure.

IV. PROTECTION METHODS

As demonstrated in the last part, vent array, joint laps, CD-ROM and the display are the main ways that EMI coupled into the enclosure. To diminish EMI coupled into the enclosure, light transmitting and electromagnetic wave shielding composite materials can be used to produce the CD-ROM shell and display screen [14-17]. Additionally, one can package CD-ROM into a metal box, or external drives may be used. Thus protection of CD-ROM and the display will not be discussed here.

In this part, we mainly focus on the programs to limit the EMI penetrated through vent array and joint laps. To limit the coupled EMI through the vent array, waveguide window is used to replace of the vent array. To limit the EMI coupled through the joint lap, rivet number is increased, the depth of the joint lap is increased and conductive gaskets are filled into the joint laps.

A. Protection of the vent array

Waveguide window, as graphed in Fig. 9, is an efficient way of letting air travel through while stopping electromagnetic wave propagating. The electromagnetic wave will vanish significantly when the wave frequency is lower than the stop frequency of the waveguide. To reduce the EMI under the frequency 40 GHz, a waveguide with sectional size 3 mm×3 mm and 15 mm in length is tested. The sectional area of the waveguide is the same as the area of the vent array on the two faces respectively.

Simulation is carried out again as the vent array is replaced by the waveguide window, and both the electric field waveform at the center and the field distribution in the enclosure are monitored.

Amplitude of the electric field component E_x is 7.8 V/m, and field component amplitude is 9.1 V/m for E_y and 23.0 V/m for E_z respectively. In Fig. 10 (a) is graphed the waveform of the electric field component E_z .

It is clear that the coupled EMI into the enclosure is greatly reduced when the vent array are replaced by the waveguide window.

The total electric field distribution in the enclosure is graphed in Fig. 10 (b), and location of the waveguide window is obvious. Compared with Fig. 4 (b), it is clear that the coupled EMI is greatly reduced. The amplitude of the electric field varies from 10.0 dBV/m to 66.3 dBV/m in the enclosure, and the amplitude is lower than 30 dBV/m at most areas. That means about a 20 dB decrease of SE is achieved. Thus it can be concluded that waveguide window is an efficient way to improve SE of the enclosure.

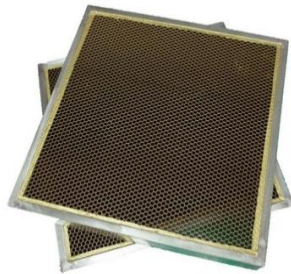
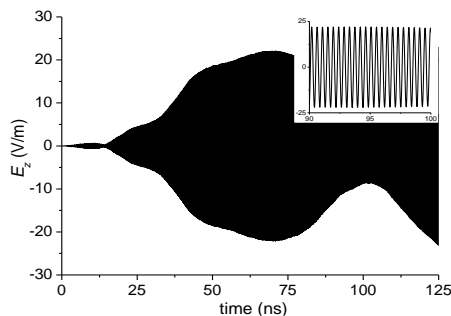
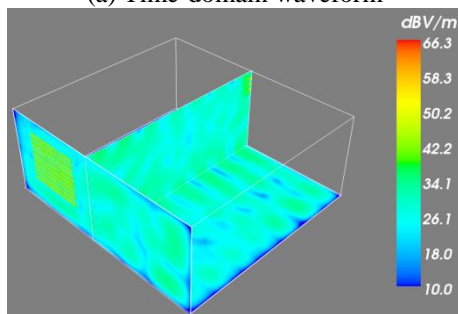


Fig. 9. Rectangular waveguide.



(a) Time-domain waveform



(b) Field distribution

Fig. 10. EMI coupled through waveguide window.

B. Protection of the joint laps

To protect the enclosure against EMI penetrated through joint laps, three methods are suggested. Firstly, the rivet number on one side of the enclosure is increased from 2 to 6, and then further to 13, as shown in Fig. 11.

Secondly, the depth of the joint laps is increased from 5 mm to 10 mm when the rivet number is 6. Thirdly, conductive gaskets are filled into the joint laps, and the width is reduced from 5 mm to 3 mm when the rivet number is 6 and the lap depth is 10 mm, as shown in Fig. 11.

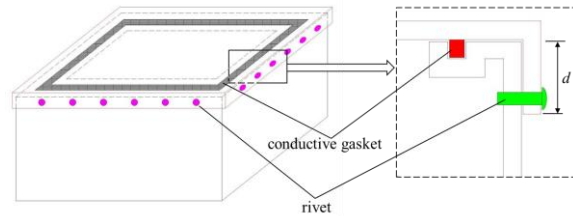
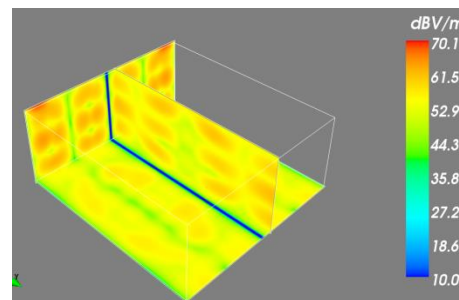
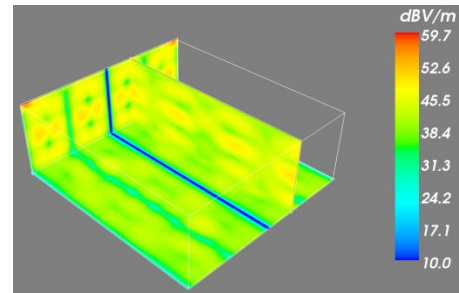


Fig. 11. Protection of joint laps.



(a) 6 rivets



(b) 13 rivets

Fig. 12. Field distribution versus rivet number.

Firstly, the rivet number is increased from 2 to 6, which means the joint laps on each side is divided into 7 short joint laps. The width and depth of the joint laps are the same as that in the last part. It is worthy of noting that the rivets are equidistantly located, and the total length of the 7 short joint laps is the same as the long joint laps of the last section. In Fig. 12 (a) is graphed the field distribution in the enclosure when 6 rivet is used, and it can be seen that there is a 5-10 dB SE improvement compared with that in Fig. 6 (b). Additionally, the rivet number is further increased to 13, and the field distribution is presented in Fig. 12 (b). It is clear another 10 dB SE improvement is achieved when 13 rivets are used.

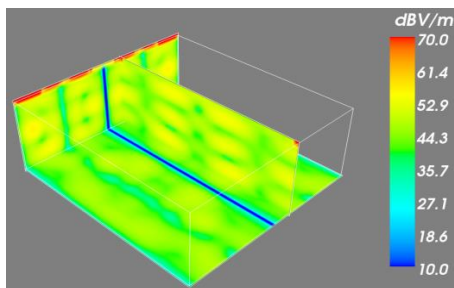


Fig. 13. Field distribution as the joint lap enlarged.

Secondly, the joint laps depth d is increased from 5 mm to 10 mm when 6 rivets are used, and the joint lap width is the same. The field distribution is presented in Fig. 13, and it can be seen that SE of the enclosure is improved 5-10 dB compared with that shown in Fig. 12 (a).

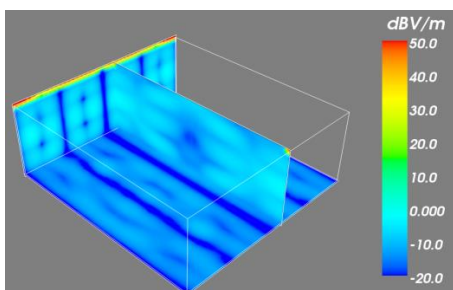


Fig. 14. Field distribution when joint laps is filled by conductive gaskets.

Thirdly, the joint laps are filled with conductive gaskets. Here the joint lap width is supposed to be reduced from 0.5 mm to 0.3 mm when conductive gaskets are filled, and the depth is 10 mm while 6 rivets are used. The field distribution is graphed in Fig. 14. It is clear that SE is greatly improved, and the coupled electric field is under 10 dBV/m at most areas except the areas adjacent to the joint laps.

From the analyses above, it can be concluded that increasing the rivet number, enlarging the joint laps depth, and filling conductive gaskets are all efficient ways to improve the SE of the enclosure.

V. CONCLUSIONS

In this paper, some suggested methods are studied to improve SE of the computer enclosure. Firstly, the slots on the enclosure are divided into five types and the coupled EMI into the enclosure is simulated when only one type slots exists. From comparison of both the electric field waveform and the field distribution in the enclosure, vent array, joint laps, CD-ROM and display are found to be the main ways that EMI coupled into the enclosure. Secondly, some suggested methods are

presented to reduce the coupled EMI. Waveguide window can be used to replace of the vent array. To reduce the coupled EMI through the joint laps, rivet number and the depth of the joint laps can be increased, and conductive gaskets can be filled into the joint laps. From numerical analyses, it can be demonstrated that the proposed methods are efficient ways to improve the SE of the computer enclosure.

ACKNOWLEDGMENT

This work was supported in part by the School Foundation under Grant No. FD201506.

REFERENCES

- [1] T. Cvetković, V. Milutinović, N. Dončov, and B. Milovanović, "Numerical investigation of monitoring antenna influence on shielding effectiveness characterization," *ACES Journal*, vol. 29, no. 11, pp. 837-846, 2014.
- [2] M. R. Barzegaran and O. A. Mohammed, "Computational electromagnetics for the evaluation of EMC issues in multi-component energy systems," *ACES Journal*, vol. 29, no. 12, pp. 1077-1092, 2014.
- [3] W. A. Radasky, C. E. Baum, and M. W. Wik, "Introduction to the special issue on high-power electromagnetics (HPEM) and intentional electromagnetic interference (IEMI)," *IEEE Trans Electromagnetic Compatibility*, vol. 46, pp. 314-321, 2004.
- [4] W. Abdelli, X. Mininger, L. Pichon, and H. Trabelsi, "Impact of composite materials on the shielding effectiveness of enclosures," *ACES Journal*, vol. 27, no. 4, pp. 369-374, 2012.
- [5] A. Taflov and S. C. Hagness, *Computational Electrodynamics: The Finite-Difference Time-Domain Method*. 3rd ed., Artech House, 2005.
- [6] A. Capozzoli, O. Kilic, C. Curcio, and A. Liseno, "The success of GPU computing in applied electromagnetics," *ACES Journal*, vol. 1, no. 4, pp. 113-116, 2016.
- [7] M. F. Hadi, "Wide-angle absorbing boundary conditions for low and high-order FDTD algorithms," *ACES Journal*, vol. 24, no. 1, pp. 9-15, 2009.
- [8] G. Liu, "Time-domain electromagnetic inversion technique for biological tissues by reconstructing distributions of Cole-Cole model parameters," *ACES Journal*, vol. 32, no. 1, pp. 8-14, 2017.
- [9] A. V. Brovko, E. K. Murphy, and V. V. Yakovlev, "Waveguide microwave imaging: Solids volume fraction of particulate materials," *ACES Journal*, vol. 30, no. 11, pp. 1161-1167, 2015.
- [10] R. Xiong, B. Chen, N.-H. Zhou, et al., "A new computational model for the FDTD analysis of

sub-structures on infinite plates,” *ACES Journal*, vol. 28, no. 1, pp. 41-48, 2013.

- [11] D. W. Sun and J. H. Yu, “Extending the 2-D contour path method to the 3-D,” *ACES Journal*, vol. 10, pp. 655-657, 2011.
- [12] J. P., Berenger, “A perfect matched layer for the absorption of electromagnetic waves,” *Journal of Computational Physics*, vol. 114, pp. 110-117, 1996.
- [13] J. A. Roden and S. D. Gedney, “Convolution PML (CPML): An efficient FDTD implementation of the CFS-PML for arbitrary media,” *Microwave and Optical Technology Letters*, vol. 27, no. 5, pp. 334-339, Dec. 2000.
- [14] K. Matumura, Y. Kagawa, and K. Baba, “Light transmitting electromagnetic wave shielding composite materials using electromagnetic wave polarizing effect,” *Journal of Applied Physics*, vol. 101, no. 1, pp. 4270-4339, Dec. 2000.
- [15] H. Shao, J. Guan, and Y. Wang, “Development of electromagnetic shielding composite materials,” *Safety & EMC*, vol. 27, no. 1, pp. 334-339, 2008.
- [16] M. S. Sarto, F. Sarto, M. C. Larciprete, et al., “Nanotechnology of transparent metals for radio frequency electromagnetic shielding,” *IEEE Transactions on Electromagnetic Compatibility*, vol. 45, no. 4, pp. 586-594, 2003.
- [17] W. M. Kim, D. Y. Ku, I.-K. Lee, et al., “The electromagnetic interference shielding effect of indium-zinc oxide/silver alloy multilayered thin films,” *Thin Solid Films*, vol. 473, pp. 315-320, 2005.



Run Xiong was born in Sichuan Province, China, in 1983. He received the B.S., M.S. and Ph.D. degrees in Electric Systems and Automation from PLA University of Science and Technology, Nanjing, China, in 2005, 2010 and 2014 respectively. He is now with the National Key Laboratory on Electromagnetic Environment and Electro-optical Engineering, and his research interests include computational electromagnetics and EMC.



Wen Yang was born in Tongren, Guizhou, China, in 1982. He received B.S. degree in Electric Systems and its Automation from Nanjing Engineering Institute, China, in 2005. Currently, he is a Pioneer Engineer with the Army Research Institute of PLA, Kunming, Yunnan. His current research interest is computational electromagnetics and the electric system design.



Yan-Tao Duan was born in Hebei, China, in 1980. He received the B.S., M.S., and Ph.D. degrees in Electric Systems and Automation from the Nanjing Engineering Institute, Nanjing, China, in 2002, 2006, and 2010, respectively. He is currently a Lecturer with the National Key Laboratory on Electromagnetic Environmental Effects and Electro-optical Engineering, Army Engineering University of PLA, Nanjing, China. His research interests include computational electromagnetics, lightning, and EMP.